



HAL
open science

Observation of a Resonant Four-Body Interaction in Cold Cesium Rydberg Atoms

J. Gurian, P. Cheinet, Paul Huillery, A. Fioretti, J. Zhao, P. Gould, D. Comparat, P. Pillet

► **To cite this version:**

J. Gurian, P. Cheinet, Paul Huillery, A. Fioretti, J. Zhao, et al.. Observation of a Resonant Four-Body Interaction in Cold Cesium Rydberg Atoms. *Physical Review Letters*, 2012, 108 (2), pp.023005. 10.1103/PhysRevLett.108.023005 . hal-04291820

HAL Id: hal-04291820

<https://hal.science/hal-04291820v1>

Submitted on 17 Nov 2023

HAL is a multi-disciplinary open access archive for the deposit and dissemination of scientific research documents, whether they are published or not. The documents may come from teaching and research institutions in France or abroad, or from public or private research centers.

L'archive ouverte pluridisciplinaire **HAL**, est destinée au dépôt et à la diffusion de documents scientifiques de niveau recherche, publiés ou non, émanant des établissements d'enseignement et de recherche français ou étrangers, des laboratoires publics ou privés.

Observation of a Resonant Four-Body Interaction in Cold Cesium Rydberg Atoms

J. H. Gurian,¹ P. Cheinet,¹ P. Huillery,¹ A. Fioretti,¹ J. Zhao,^{1,2} P. L. Gould,^{1,3} D. Comparat,¹ and P. Pillet¹

¹Laboratoire Aimé Cotton, CNRS, Univ Paris-Sud, Bâtiment 505, 91405 Orsay, France

²State Key Laboratory of Quantum Optics and Quantum Optics Devices, College of Physics and Electronics Engineering, Shanxi University, Taiyuan 030006, China

³Department of Physics, University of Connecticut, Storrs, Connecticut 06269-3046, USA

(Received 6 September 2011; published 11 January 2012)

Cold Rydberg atoms subject to long-range dipole-dipole interactions represent a particularly interesting system for exploring few-body interactions and probing the transition from 2-body physics to the many-body regime. In this work we report the direct observation of a resonant 4-body Rydberg interaction. We exploit the occurrence of an accidental quasicoincidence of a 2-body and a 4-body resonant Stark-tuned Förster process in cesium to observe a resonant energy transfer requiring the simultaneous interaction of at least four neighboring atoms. These results are relevant for the implementation of quantum gates with Rydberg atoms and for further studies of many-body physics.

DOI: 10.1103/PhysRevLett.108.023005

PACS numbers: 32.80.Ee, 34.50.Cx

The physics of atomic systems at low densities ($n \leq 10^{13} \text{ cm}^{-3}$) can generally be described in terms of the action of electromagnetic fields and binary (2-body) interactions. However, a number of interesting effects arise when few-body or many-body interactions come into play. Notable examples include 3-body recombination [1–3], leading to molecule formation in optical or magnetic traps, trimer photoassociation [4], and Efimov physics, leading to trimers and more recently tetramer formation [5–8].

Cold, highly excited (Rydberg) atoms [9–11] are a promising playground for many-body interactions, due to their strong and long-range interactions together with the long interaction times available in a cold sample. This was first revealed in studies [12,13] on the broadening of Rydberg energy transfer resonances. Subsequent work further explored the broadening mechanisms [11,14–18], the influence of the system dimensionality [18], and dephasing [19]. A renewed interest in cold Rydberg systems has recently been triggered by their possible use in quantum computation [20]. Long-range van der Waals [21] or dipole-dipole [22,23] interactions allow control of the atomic excitation in a given volume, the so-called blockade effect, enabling the implementation of quantum gates [24,25]. In this respect, a careful control over the number of contributing partners is necessary as 3-body and 4-body effects could be large enough to interfere with the computation process [26].

Another key feature of cold Rydberg atoms is the ability to tune interactions by simply using an external electric field. In the process known as a Förster resonance, the energy of the final many-body state can be Stark tuned into resonance with the initial state, leading to a resonant energy transfer (FRET) [27,28]. In this case, modeling the system requires including multiple atoms and solving the full three-dimensional many-body wave equation [18,29].

However, the number of atoms which must be included for accurate results is still unclear [30–32]. It is therefore important to study cases where a small number of atoms play a dominant role. This is the case in the striking experiments on 3- or 4-body recombination [6–8], where the few-body process is characterized by a resonant loss mechanism.

In this Letter we present first results on a 4-body energy transfer process due to a 4-body Stark-tuned FRET resonance occurring in cesium at an electric field of 79.99 V/cm:

$$4 \times 23p_{3/2} \rightarrow 2 \times 23s + 23p_{1/2} + 23d_{5/2}. \quad (1)$$

We take advantage of two nearly resonant Cs 2-body Stark-tuned FRET resonances,

$$23p_{3/2} + 23p_{3/2} \rightarrow 23s + 24s, \quad (2)$$

$$24s + 24s \rightarrow 23p_{1/2} + 23d_{5/2}, \quad (3)$$

occurring, respectively, at 79.94 V/cm and 80.42 V/cm. All states have $|m_J| = 1/2$ unless specified otherwise. For convenience, the states $23p_{3/2}$, $23s$, $24s$, $23p_{1/2}$, and $23d_{5/2}$ are labeled as p , s' , s , p' , and d , respectively. The three resonances are illustrated in Fig. 1 and are denoted as $p \rightarrow d$ [Eq. (1)], $p \rightarrow s$ [Eq. (2)], and $s \rightarrow d$ [Eq. (3)]. Observing d population after exciting the p state is the signature that four atoms exchanged energy.

The experimental setup consists of a standard Cs magneto-optical trap (MOT) at the center of four parallel 60 mm by 130 mm wire mesh grids of 80 μm thickness and 1 mm grid spacing. The center pair of grids is spaced by 1.845 ± 0.01 cm, and the outer grids are 1.5 cm from the inner grids. Voltages up to ± 5 kV can be applied arbitrarily to the four grids. Six additional small electrodes surround the excitation region at the grid edges to cancel stray fields. The central grid spacing has been calibrated by

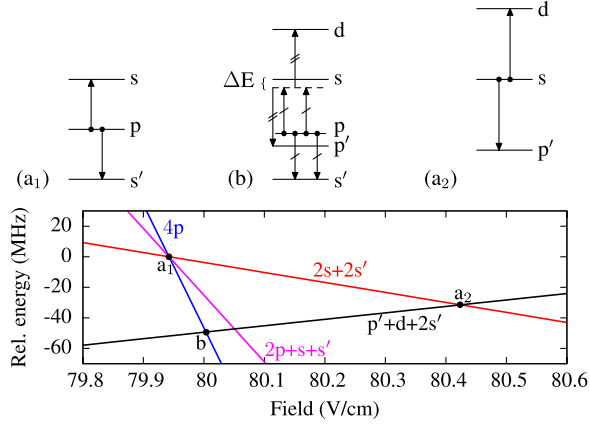


FIG. 1 (color online). Calculated four-atom energy for the two relevant 2-body resonances (a_1) and (a_2) and the $p \rightarrow d$ 4-body resonance (b) as a function of the electric field.

measuring Stark shifts of the $23p$ and $22d$ states for fields up to 100 V/cm and comparing them to theory [33].

The trapped atoms are excited to a Stark-shifted Rydberg state, nl , using the MOT light and two additional lasers via the scheme: $6s \rightarrow 6p \rightarrow 7s \rightarrow nl$. The $6p \rightarrow 7s$ step uses a 1470 nm, 10 mW laser frequency-locked on a Doppler-free feature in a Cs cell excited by resonant $6s \rightarrow 6p$ light. In order to avoid perturbations of the atomic cloud, the 1470 nm laser is switched on for only 500 ns, at a 10 Hz repetition rate, by an acousto-optical modulator (AOM). The first order AOM output is focused to a 400 μm diameter spot at the atomic sample and its intensity is chosen to avoid power-broadening the transition. A cw Ti:sapphire ring laser, providing roughly 1.8 W at ≈ 795 nm, drives the $7s \rightarrow nl$ transition. This laser is switched in the same manner and the beam is focused to a 300 μm spot diameter and perpendicularly overlapped with the 1470 nm beam in the atomic sample. The simultaneous 500 ns pulses are short enough to avoid excitation blockade. We thus excite a Gaussian cloud of up to $2 \times 10^5 p$ atoms, 260 μm in diameter, with a maximum peak density, ρ_p , of $9 \times 10^9 \text{ cm}^{-3}$.

Selective field ionization is used to measure the populations of the various Rydberg states. A voltage ramp is applied to one of the grids, 1.5 μs after the beginning of the laser excitation, rising to 4.3 kV in 4 μs . The resultant ions are detected by a microchannel plate (MCP) detector, 210 mm from the center of the trapped cloud. The amplitude of the field ionization pulse is chosen to optimally isolate the d time-of-flight (TOF) from the other signals, as displayed in Fig. 2, where each state has been excited directly in a nonresonant electric field. We use the time gates shown to measure the population of each state.

It is important in this experiment to retrieve the correct populations of the p , s , and d states from a single TOF signal. As one can see in Fig. 2, we have the ability to differentiate these Rydberg states, but it is also apparent

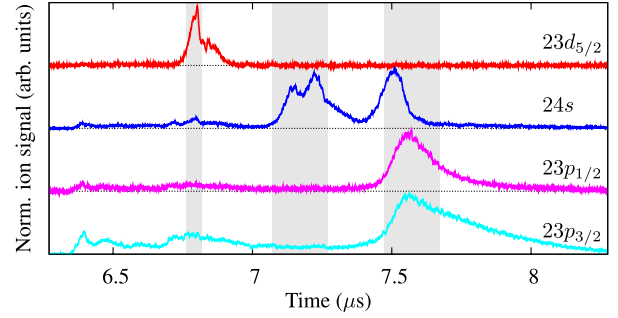


FIG. 2 (color online). Thirty-shot-averaged normalized time-of-flight signals for laser excitation to the Stark-mixed d , s , p' and p states. The four traces have been vertically offset for clarity, with the respective zero levels shown as horizontal dashed lines. The electric field is set to 79 V/cm, far from any FRET resonance. The gates for the d , s , and p signals are shown as gray shaded regions.

that they are not cleanly separated into their respective gates, for example, due to blackbody radiation or multiple ionization pathways. We therefore use traces, shown in Fig. 2, where each state is separately excited and the electric field is not resonant, to quantify the cross talk between the various gates. We also account for the detection efficiency of each state, using a voltage which ionizes completely, and separately measuring the global MCP detection efficiency. We notice a slight overestimation of the measured cross talk coefficients leading to negative s or d population for small p excitation. We correct these coefficients and these corrections are included in the error bars shown in the experimental figures below. Throughout the Letter, the recorded signals are converted to the actual number of atoms in each state via the matrix,

$$\begin{pmatrix} d \\ s \\ p \end{pmatrix} = \begin{pmatrix} 2.016 & -0.0644 & -0.082 \\ -0.100 & 4.645 & -0.275 \\ 0.083 & -3.147 & 4.149 \end{pmatrix} \begin{pmatrix} d \\ s \\ p \end{pmatrix}_{\text{gate}}, \quad (4)$$

whose off-diagonal elements characterize the cross talk. Fortunately, the d -state signal has minimal cross talk with the others, and a more advanced signal analysis [34] is not required.

Although 2-body Stark-tuned FRET resonances have been observed previously [12,22], we present them below for completeness. We first verify the 2-body $p \rightarrow s$ resonance, as shown in Fig. 3(a). The resonance is observed at 79.94 V/cm, and the flat-top resonance shape suggests that the transition is saturated. We observe a small field inhomogeneity in our experimental region, which we estimate to be around 5 V/cm/cm, via broadening of the p laser excitation line. This corresponds to ± 0.05 V/cm in the excitation volume, which is thus the electric field measurement resolution. Stark field laser excitation of the s state lets us measure the 2-body $s \rightarrow d$ resonance, as shown in Fig. 3(b). We can excite up to 1.4×10^5 $24s$ atoms at a

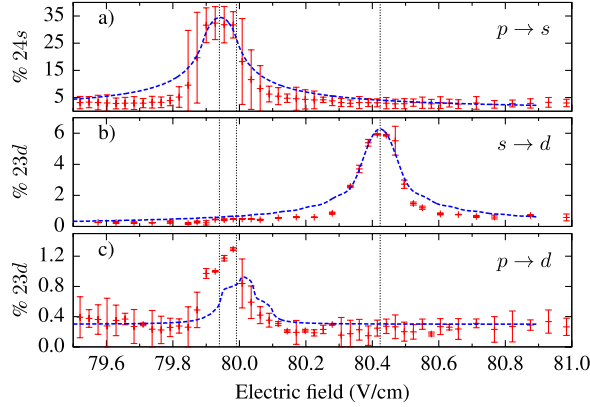


FIG. 3 (color online). Number of detected Rydberg atoms as a function of applied electric field. (a) percentage of detected s atoms when exciting the p state. (b) percentage of d detected when exciting the s state. (c) percentage of d detected when exciting the p state. The error bars account for the corrections to the cross talk coefficients, which are larger for s than for d , and for the observed field inhomogeneity that affects more the p excitation, leading to larger error bars than in the s excitation case. The results of our calculation for four equidistant atoms are overlaid as dashed blue lines, with the $p \rightarrow s$ calculation amplified by a factor of 2 and the $s \rightarrow d$ divided by a factor of 3 to coincide with experimental results. The three resonant field values are illustrated by the vertical dotted lines.

peak density, ρ_s , of $8 \times 10^9 \text{ cm}^{-3}$. The $s \rightarrow d$ resonance is observed at 80.42 V/cm. We have used the Cs energy levels published by Sansonetti [35] for our calculations. Unfortunately, the $24p_{3/2}$ state energy uncertainty (0.03 cm^{-1}) creates a large uncertainty in the position of the 2-body resonances; $\pm 0.1 \text{ V/cm}$ for the $p \rightarrow s$ transition, and $\pm 1 \text{ V/cm}$ for the $s \rightarrow d$ transition. While the positions of the resonances are not well defined, the slopes shown in Fig. 1 are stable to within 0.1%, and we have therefore aligned the calculated 2-body resonances with our experimentally measured positions.

Once the 2-body resonances have been measured, the location of the 4-body resonance is accurately known. We observe greater than 1% $p \rightarrow d$ transfer with a peak at 79.99 V/cm, as shown in Fig. 3(c). While the 4-body resonance partially overlaps the $p \rightarrow s$ 2-body resonance in field, it is important to recall that the d state signal is well separated in the TOF.

To provide insight into the 4-body resonance, we have developed a minimal toy model with four equidistant atoms arranged as a tetrahedron. The four possible states $|pppp\rangle$ (initial state), $|ss'pp\rangle$, $|ss'ss'\rangle$, and $|ds'p's'\rangle$ (detected state) are coupled by dipole-dipole interactions, calculated between the in-field eigenstates of the Rydberg atoms [33]. The final populations, shown in Fig. 3 as the blue dashed curves, are calculated using the density matrix and the experimental peak density and field inhomogeneity. We average the results assuming an Erlang (nearest neighbor) distribution for the 2-body distance

between the atoms, and a cubic Erlang distribution for the 4-body case. Such a 2-body model is not expected to precisely match the experiment [18] and the calculated 2-body $p \rightarrow s$ curve is amplified by a factor of 2 while the $s \rightarrow d$ curve has been diminished by a factor of 3 to match the experimentally observed results. To account for the 0.3% background observed in the $p \rightarrow d$ 4-body transfer, the 4-body curve baseline has been shifted accordingly. While a more detailed many-body calculation would be needed to reproduce the data [29], it is remarkable that such a crude 4-body calculation qualitatively reproduces the shape of the experimental signal.

The observation of d state population constitutes a clear, direct signature of an interaction involving at least four bodies. The strong signature that the process is not a simple combination of two consecutive 2-body processes, but a genuine 4-body process, lies in the relative strengths of the d transfer at the 4-body resonance field when initially exciting the p or s state. Figure 4(a) shows the number of detected d atoms for comparable densities of s , either excited directly (1.4×10^5) or obtained from exciting p and allowing 2-body transfer into s ($< 10^5$). The larger number of detected d atoms (about a factor of 4) when exciting p , despite a smaller s density, is explained by the fact that here the 4-body $p \rightarrow d$ transfer is resonant whereas the 2-body $s \rightarrow d$ transfer is not. Finally, exciting the p state in the $|m_j| = 3/2$ case, where the $p \rightarrow s$ resonance lies around 88.1 V/cm and the 4-body resonance is well separated from both 2-body resonances, we see in Fig. 4(b) that no significant d population is detected at the $p \rightarrow s$ resonance. The small observed signal is

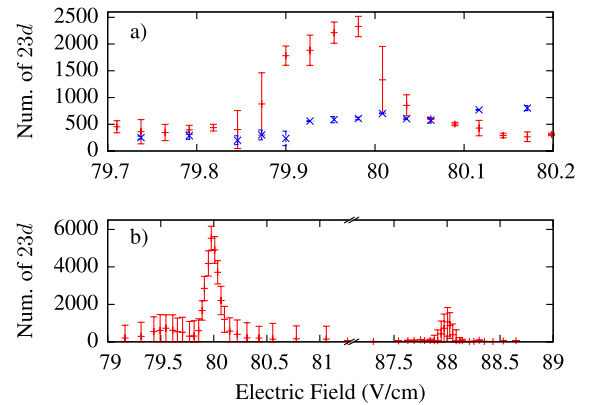


FIG. 4 (color online). Figure (a) shows the number of detected d atoms as a function of the applied electric field for exciting the p (red +) and s (blue \times) states, with an s density comparable or greater in the s excitation than in the p excitation. The on-resonant 4-body process creates more than a factor of 4 more d atoms than the off-resonant $s \rightarrow d$ 2-body process at 79.99 V/cm. Figure (b) shows the number of detected d atoms when exciting the $p \rightarrow s$ resonance for the $|m_j| = 1/2$ (79.94 V/cm) and $|m_j| = 3/2$ (88.14 V/cm). We observe no significant d state population in the $|m_j| = 3/2$ case.

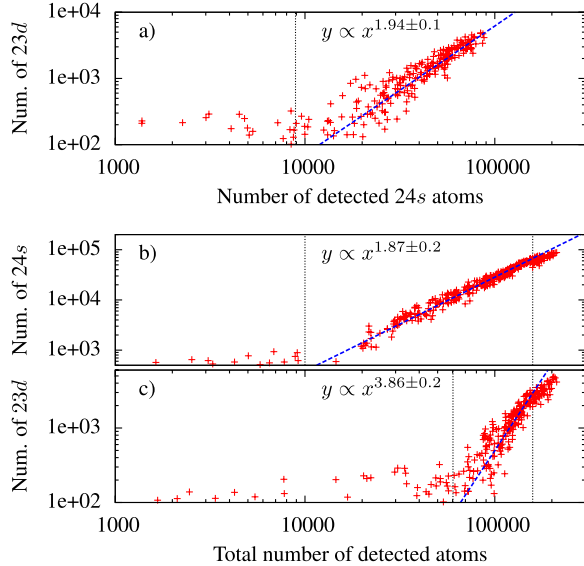


FIG. 5 (color online). Number of detected Rydberg atoms as the intensity of the Rydberg excitation laser is varied. (a) Number of d atoms as a function of s detected atoms. (b) Number of detected s atoms as a function of the total number of detected Rydberg atoms. (c) Number of d atoms created vs the total number of detected Rydberg atoms. Best fits below 1.6×10^5 atoms (demarcated with a vertical dotted line) are shown as the dashed blue lines.

compatible with the estimated error on the inversion matrix coefficients in Eq. (4).

A way to increase the population transfer is to shift the applied field from the $p \rightarrow s$ resonance to the $s \rightarrow d$ resonance between laser excitation and detection. The two 2-body FRETs are then consecutively resonant and we should get a d transfer comparable to that obtained when exciting s directly. Indeed, we have observed up to 7.5% $p \rightarrow d$ population transfer with a 0.6 V/cm field shift, confirming that the $p \rightarrow s$ population transfer at 79.94 V/cm leads to about the same s density as direct s excitation. With a larger shift it is also possible to induce a transfer to d from the $|m_j| = 3/2p$ state. We observed up to 2.1% $p \rightarrow d$ population transfer with a -7.7 V/cm field shift starting from 88.14 V/cm.

The field inhomogeneity and the proximity of the 4-body and 2-body FRET resonances impede further studies on the resonance shape. Nevertheless, having identified the 4-body resonance, we can study the transfer dependence on the initial p Rydberg atom density. We vary this density by attenuating the Rydberg excitation laser with a set of neutral density filters, sitting on the 79.99 V/cm $p \rightarrow d$ resonance. The results are shown in Fig. 5. We have fit data only above the detection sensitivity of 500 atoms for s and 100 atoms for d . The population transfer from the initial p state to the s state is shown in Fig. 5(b). It increases as ρ_p^2 until the $p \rightarrow s$ transfer starts saturating above 1.6×10^5 atoms, as expected from Fig. 3, and we have

limited all three fits to below this value. The d state population transfer as a function of the detected s population is shown in Fig. 5(a). The quadratic, i.e., nonlinear, dependence ensures us of the correct data treatment presented in Eq. (4). Finally, we observe in Fig. 5(c) the number of detected d atoms as a function of the total number of excited Rydberg atoms. We clearly see the influence of the s transfer saturation on the d transfer. Nevertheless, we can see the d population transfer scaling as ρ_p^4 , again demonstrating that d state observation links to a 4-body process.

In conclusion, we have observed a 4-body interaction between Rydberg atoms excited in a MOT. The observed process is a FRET involving the simultaneous interaction of at least four neighboring partners. Its occurrence depends on the electric field proximity of the parent 2-body FRET resonances and to the quasicoincidence of the 4-body resonance with one of them. We have studied the 4-body reaction as a function of the electric field and the initial Rydberg density by selectively detecting the reaction products.

Tunable FRET resonances are extremely interesting tools for making Rydberg atoms into suitable systems for quantum information storage and processing [11,20]. Nevertheless, care should be taken to properly evaluate the occurrence of higher-order (3-body, 4-body, or n -body) processes when issues of fidelity and decoherence are to be addressed.

This work on a strong 4-body interaction is an important step towards studying few-body and many-body effects in dilute gases. Such processes which go beyond the 2-body interaction are likely to occur for many Rydberg states, especially at the larger densities that can be obtained in optical traps. For instance, other 4-body FRET resonances exist for four nonidentical Rydberg atoms, for which the resonance field is better separated from the 2-body resonance field. Furthermore, the use of optical lattices to induce spatial order in the system should allow new insights into the physics of novel quantum systems.

This work has been supported by the *Institut francilien de recherche sur les atomes froids* (IFRAF). J. G. and A. F. have been supported by the “*Triangle de la Physique*” under Contract No. 2007-n.74T and No. 2009-035T GULFSTREAM. P.G. has been supported by the “*Triangle de la Physique*” under Contract No. 2010-026T COCORYCO. J.Z. has been supported by the NSFC under Grant No. 61078001.

-
- [1] S. Jochim, M. Bartenstein, A. Altmeyer, G. Hendl, C. Chin, J.H. Denschlag, and R. Grimm, *Phys. Rev. Lett.* **91**, 240402 (2003).
 [2] T. Weber, J. Herbig, M. Mark, H.-C. Nägerl, and R. Grimm, *Phys. Rev. Lett.* **91**, 123201 (2003).

- [3] B. D. Esry, C. H. Greene, and J. P. Burke, *Phys. Rev. Lett.* **83**, 1751 (1999).
- [4] V. Bendkowsky, B. Butscher, J. Nipper, J. B. Balewski, J. P. Shaffer, R. Löw, T. Pfau, W. Li, J. Stanojevic, T. Pohl, and J. M. Rost, *Phys. Rev. Lett.* **105**, 163201 (2010).
- [5] J. von Stecher, J. D’Incao, and C. Greene, *Nature Phys.* **5**, 417 (2009).
- [6] F. Ferlaino, S. Knoop, M. Berninger, W. Harm, J. P. D’Incao, H.-C. Nägerl, and R. Grimm, *Phys. Rev. Lett.* **102**, 140401 (2009).
- [7] N. Gross, Z. Shotan, S. Kokkelmans, and L. Khaykovich, *Phys. Rev. Lett.* **103**, 163202 (2009).
- [8] S. E. Pollack, D. Dries, and R. G. Hulet, *Science* **326**, 1683 (2009).
- [9] T. F. Gallagher, *Rydberg Atoms* (Cambridge University Press, Cambridge, England, 1994).
- [10] T. F. Gallagher and P. Pillet, *Adv. At. Mol. Opt. Phys.* **56**, 161 (2008).
- [11] D. Comparat and P. Pillet, *J. Opt. Soc. Am. B* **27**, A208 (2010).
- [12] I. Mourachko, D. Comparat, F. de Tomasi, A. Fioretti, P. Nosbaum, V. M. Akulin, and P. Pillet, *Phys. Rev. Lett.* **80**, 253 (1998).
- [13] W. R. Anderson, J. R. Veale, and T. F. Gallagher, *Phys. Rev. Lett.* **80**, 249 (1998).
- [14] I. Mourachko, W. Li, and T. F. Gallagher, *Phys. Rev. A* **70**, 031401 (2004).
- [15] P. J. Tanner, J. Han, E. S. Shuman, and T. F. Gallagher, *Phys. Rev. Lett.* **100**, 43002 (2008).
- [16] A. Reinhard, T. Cubel Liebisch, K. C. Younge, P. R. Berman, and G. Raithel, *Phys. Rev. Lett.* **100**, 123007 (2008).
- [17] J. Han, *Phys. Rev. A* **82**, 052501 (2010).
- [18] T. J. Carroll, S. Sunder, and M. W. Noel, *Phys. Rev. A* **73**, 032725 (2006).
- [19] W. R. Anderson, M. P. Robinson, J. D. D. Martin, and T. F. Gallagher, *Phys. Rev. A* **65**, 063404 (2002).
- [20] M. Saffman, T. G. Walker, and K. Mølmer, *Rev. Mod. Phys.* **82**, 2313 (2010).
- [21] D. Tong, S. M. Farooqi, J. Stanojevic, S. Krishnan, Y. P. Zhang, R. Côté, E. E. Eyler, and P. L. Gould, *Phys. Rev. Lett.* **93**, 063001 (2004).
- [22] T. Vogt, M. Viteau, J. Zhao, A. Chotia, D. Comparat, and P. Pillet, *Phys. Rev. Lett.* **97**, 083003 (2006).
- [23] T. Vogt, M. Viteau, A. Chotia, J. Zhao, D. Comparat, and P. Pillet, *Phys. Rev. Lett.* **99**, 073002 (2007).
- [24] A. Gaëtan, Y. Miroshnychenko, T. Wilk, A. Chotia, M. Viteau, D. Comparat, P. Pillet, A. Browaeys, and P. Grangier, *Nature Phys.* **5**, 115 (2009).
- [25] T. Wilk, A. Gaëtan, C. Evellin, J. Wolters, Y. Miroshnychenko, P. Grangier, and A. Browaeys, *Phys. Rev. Lett.* **104**, 010502 (2010).
- [26] A. Mizel and D. A. Lidar, *Phys. Rev. Lett.* **92**, 077903 (2004).
- [27] K. Afrousheh, P. Bohlouli-Zanjani, D. Vagale, A. Mugford, M. Fedorov, and J. D. D. Martin, *Phys. Rev. Lett.* **93**, 233001 (2004).
- [28] I. I. Ryabtsev, D. B. Tretyakov, I. I. Beterov, and V. M. Entin, *Phys. Rev. Lett.* **104**, 073003 (2010).
- [29] T. G. Walker and M. Saffman, *Phys. Rev. A* **77**, 032723 (2008).
- [30] M. Reetz-Lamour, T. Amthor, S. Westermann, J. Denskat, A. L. de Oliveira, and M. Weidemüller, *Nucl. Phys. A* **790**, 728c (2007).
- [31] K. C. Younge, A. Reinhard, T. Pohl, P. R. Berman, and G. Raithel, *Phys. Rev. A* **79**, 043420 (2009).
- [32] T. J. Carroll, C. Daniel, L. Hoover, T. Sidie, and M. W. Noel, *Phys. Rev. A* **80**, 052712 (2009).
- [33] M. L. Zimmerman, M. G. Littman, M. M. Kash, and D. Kleppner, *Phys. Rev. A* **20**, 2251 (1979).
- [34] V. D. Irby, R. G. Rolfes, O. P. Makarov, K. B. MacAdam, and M. I. Syrkin, *Phys. Rev. A* **52**, 3809 (1995).
- [35] J. E. Sansonetti, *J. Phys. Chem. Ref. Data* **38**, 761 (2009).